CO–LOCATED PRESSURE–CORRECTION FORMULATIONS ON UNSTRUCTURED 2–D GRIDS

N. Lambropoulos, E. S. Politis, K. C. Giannakoglou, K. D. Papailiou
Laboratory of Thermal Turbomachines,
National Technical University of Athens,
P.O. Box 64069, 15710, Athens, Greece.

1. SUMMARY

By extending a Navier-Stokes solution method for structured grids (SGs), a pressure–correction, finite–volume formulation for the numerical solution of laminar, incompressible, 2–D flows on unstructured grids (UGs) with triangular elements has been deviced. Since a co–located storage arrangement for all of the flow variables is used, the velocity and pressure fields should be artificially coupled. This is achieved through the straight-forward extension of the Pressure–Weighted Interpolation Method ($PWIM$), successfully used for SGs in the past. In the first part of the paper, the method formulation for UGs is analyzed. Then, the $PWIM$ for UGs and the boundary conditions' implementation along solid walls are investigated, on the basis of two flow problems.

2. INTRODUCTION

In incompressible flow calculations, the co–location of pressure and velocity variables is the cause of spatial decoupling in the numerically predicted pressure field. A way to suppress the pressure wiggles is by adding artificial diffusion terms in the mass conservation equation. On a SG, these terms usually consist of fourth–order pressure derivatives along the curvilinear coordinates (Rhie and Chow [6]), which result to a stabilizing five–node support stencil in each direction. The extension of the Rhie and Chow scheme to UGs is, by no means, straightforward. An alternative remedy to the same problem is through the $PWIM$, introduced by Majumdar [5], in order to compute velocities crossing the finite–volumes' boundaries which are coupled with the local pressure gradient. The momentum equations in a discrete form similar to that applied to the cell centers, but with different pressure gradient stencils, are employed to compute the aforementioned velocities. For SGs, $PWIM$ is proved to be equivalent to the Rhie and Chow scheme.

Even if the $PWIM$ can be readily applied to UGs, its equivalence with a pressure diffusion term and consequently its effectiveness needs to be investigated. This is the scope of the present paper, extending the solver for SGs described in Giannakoglou and Politis [3] and [4]. Besides, in a real UG some local pressure wiggles are likely to appear as a consequence of boundary condition implementations which fail to correctly account for the arbitrary shapes and sizes of the adjacent triangles. This issue is also addressed herein.
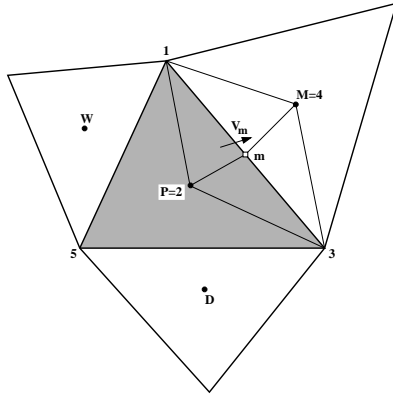
Fig. 1. Control volume in an unstructured grid of triangular elements.

The are few papers in the literature, which report on the application of the pressure–correction scheme on UGs. Thomadakis and Leschziner [8] employ semi–staggered control volumes for the momentum and the pressure–correction equations. Staggering velocities and pressure proved insufficient to suppress the pressure wiggles and consequently a small measure of artificial damping was also introduced. It is interesting to note that all of the grids studied in [8] were pseudo–UGs, where the triangles have been generated by post–processing SGs. Davidson [1] introduced a SIMPLE–like method for UGs and employed the Rhie and Chow scheme in a co–located grid arrangement. Using 'regular' UGs, the pressure wiggles were not fully eliminated.

3.   DISCRETIZATION OF THE MOMENTUM EQUATIONS

A finite–volume approximation to the momentum equations for laminar, 2–D, incompressible flows, yields

$$\int_S u_i \, (u_j n_j) \, dS = - \int_S p \, n_i \, dS + \nu \int_S \frac{\partial u_i}{\partial x_j} \, n_j \, dS, \quad i = 1, \, 2, \tag{1}$$

where u_i, $i = 1, \, 2$ stand for the Cartesian velocity components and ν is the kinematic viscosity. In eqs. (1), the repeated index convention has been used. On an UG with all flow variables stored at the barycenters of the triangular elements, the control volumes (Fig. 1) coincide with each triangle. So, in eqs. (1), S is the boundary of the cell and n_j, $j = 1, \, 2$ stand for its outward unit normal vector components.

The convection terms in eqs. (1) are computed using a second order accurate upwind scheme. According to this scheme, the convected field at the midpoint m of any grid segment separating two adjacent control volumes is calculated as

$$u_i|_m = u_i|_P + \left.\vec{\nabla} u_i\right|_P \cdot \vec{Pm}, \quad i = 1, \, 2, \tag{2}$$

where, $u_i|_P$ and $\left.\vec{\nabla} u_i\right|_P$, $i = 1, \, 2$, stand for the velocity components and their gradient at the barycenter P of the cell lying upwind of m, the criterion being the velocity vector at m. $\vec{Pm}$ is the vector connecting P and m (Fig. 1). The velocity gradients at the cell barycenters are computed by applying the Gauss theorem. This computation requires the velocity values at the cell vertices, which are obtained by scatter–adding contributions from the surrounding nodes.

For the dicretization of the diffusive fluxes through the boundaries of any control volume, a four–node stencil is employed. It is formed by the two nodes/edges of each segment (1 and 3, in Fig. 1) and the two barycenters of the adjacent triangles (2 and 4, in the same figure). By employing the Gauss theorem over (1234) we get

$$\left.\frac{\partial u_i}{\partial x_j}\right|_m = \frac{(-1)^{j-1}}{2\,(1234)} \sum_{k=1}^{4} u_i \left(x_m|_{k-1} - x_m|_{k+1} \right), \quad i,\, j = 1,\, 2, \quad m = 2\,/j, \tag{3}$$

where (1234) stands for the area of the quadrilateral. Finally, in order to compute the pressure terms in eqs. (1), pressure values at the midfaces are to be calculated by averaging the computed values at the adjacent barycenters.

By virtue of eqs. (2) and (3), the discretized form of eqs. (1) for any node P reads

$$-A_P\, u_{i\,P} + \sum_{k=1}^{3} A_{i\,k}\, u_{i\,k} + C_i = 0, \quad i = 1,\, 2, \tag{4}$$

where the summation is taken over its (three, in general) neighbours. The source terms C_i, $i = 1,\, 2$ include contributions from any other node and the pressure gradient terms. Introducing the under–relaxation parameter ω, a delta–formulation of eqs. (4) gives

$$\delta u_{i\,P}^{[m+1]} = \frac{\omega}{A_P} \left(R_i + \sum_{k=1}^{3} A_{i\,k}\, \delta u_{i\,k}^{[m]} \right), \quad i = 1,\, 2. \tag{5}$$

The Jacobi scheme is used to solve eqs. (5) and provides a provisional velocity field u_i^*, $i = 1,\, 2$, which, in general, does not satisfy the continuity equation. In eqs. (5), $[m]$ is the Jacobi iteration index.

4. THE PRESSURE–CORRECTION EQUATION

To obtain a divergence–free velocity field, a pressure–correction equation is formed and solved. The so–called p' field is used to iteratively update the pressure and the velocity fields. The pressure–velocity coupling is enforced through the straightforward extension of the *PWIM* to *UGs*. A relevant discussion will be taken up in a subsequent section.

According to the *PWIM*, it is assumed that the provisional velocity field satisfies the discretized momentum equations at both the cell barycenters and the midfaces. Consequently, at the midface m of a triangular cell, eqs. (4) still hold and read

$$u_{i\,m}^* = \frac{\omega}{A_m} \left\{ \sum_{k=1}^{3} A_{i\,k}\, u_{i\,k}^* + S_i{}' \right\}_m - \frac{\omega}{A_m} \int_{(1234)} p\, n_i\, dS + (1-\omega)\, \overline{u}_{i\,m}{}^{(n)}, \quad i = 1,\, 2, \tag{6}$$

where the area (1234) is shown in Fig. 1. Also, $S_i{}'$, $i = 1,\, 2$ stand for the C_i, $i = 1,\, 2$ source terms excluding the pressure gradient terms, considered separately in eqs. (6). The superscript (n) denotes velocities at the previous iteration level.

In order to form the pressure–correction equation, the continuity equation is integrated over the triangular elements

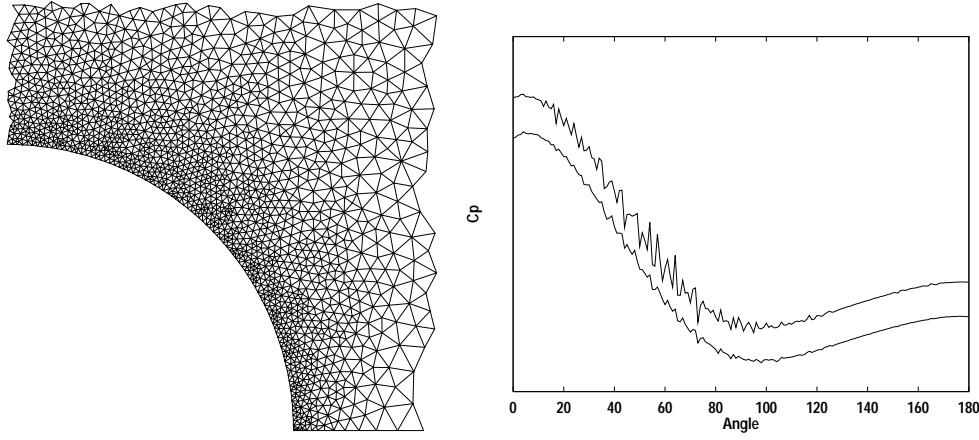$$\int_S u_j\, n_j\, dS = 0 \tag{7}$$

Fig. 2. Detail of the real UG and computed wall–pressure distributions for $TC1$, $Re = 20$.

and it is also assumed that

$$F_m = F_P \, g_m + F_M \, (1 - g_m), \tag{8}$$

where F_m may stand for $\frac{1}{A_m}$, $\left\{ \sum_{k=1}^3 A_{i\,k} \, u_{i\,k}^* + S_i' \right\}_m$, or $u_{i\,m}^{(n)}$, $\quad i = 1, 2$. In these equations, g_m is the geometrical interpolation coefficient.

As in momentum equations, the Jacobi iterative scheme is used to solve for p'. Then, the pressure field is updated as $p^{(n+1)} = p^{(n)} + p'$. The velocity components at both cell barycenters and midfaces are also updated according to

$$u_{i\,P\,or\,m}^{(n+1)} = u_{i\,P\,or\,m}^* - \frac{\omega}{A_{P\,or\,m}} \int_{S\,or\,S'} p' \, n_i \, dS \quad i = 1, 2. \tag{9}$$

5.   IMPLEMENTATION OF SOLID WALL BOUNDARY CONDITIONS

Along the solid walls, a zero Neumann boundary condition for the pressure ($dp/dn = 0$) is imposed. This condition links the pressure values calculated at the adjacent triangles' barycenters to the midpoint values of the boundary segments. In a 'real' UG, the triangles sharing an edge with the wall are arbitrarily shaped. A simple way to compute the pressure over a boundary node or a boundary segment midpoint is to consider it as equal to the pressure at the barycenter of the 'nearest' triangle in the normal direction. This is a low-order accurate scheme that results to intense wiggles in the wall–pressure distribution. These are communicated to the interior of the flowfield, as well. To demonstrate this effect, the steady flow past a cylinder ($TC1$), for $Re_d = 20$ (d is the diameter) has been examined. Using the 'real' UG shown in Fig. (2), a non–smooth pressure distribution (the one with the larger wiggles) is obtained, as shown in the same figure.

Treating the triangle, which is in contact to the wall, as a quadratic element improves a lot the pressure decoupling problem. Assume that for the triangle 123 shown in Fig. 3, which also 'contains' the normal to the wall direction at the node 1, the pressure values at the grid nodes 2 and 3 and the midfaces 4, 5 and 6 have been computed by scatter-adding computed pressures at the barycenters of the surrounding triangles. If $k = (3M)/(32)$ then it can be proved that the Neumann type boundary condition at 1 reads

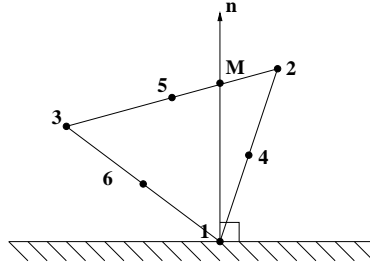$$-3p_1 - kp_2 + (k-1)p_3 + 4kp_4 + 4(1-k)p_6 = 0 \tag{10}$$

Fig. 3. Numerical implementation of solid wall boundary conditions.

This relation can be solved for p_1 to update the wall pressure values. Using this relation, the wall–pressure distribution is much smoother (see Fig. 2), though without entirely suppressing the wiggles. Finally, the wiggles can be entirely suppressed if a layer of 'structured' triangles is used to cover the solid walls. In the so–called hybrid UG the wiggles are eliminated, but the presentation of the corresponding results is deferred to a subsequent section.

6.   THE *PWIM* ON UGs
6.1   Theoretical Formulation

The application of the $PWIM$ on a 1–D node arrangement (see Fig. 4) is equivalent to adding a fouth–order pressure diffusion term to the continuity equation. So, the conservation of mass in the cell $[\beta\,\gamma]$ reads

$$u_\gamma - u_\beta = \overline{u}_\gamma - \overline{u}_\beta - \frac{D}{4}\left.\frac{\partial^4 p}{\partial x^4}\right|_B, \tag{11}$$

where overbars denote averaged values over the surrounding nodes and D is an appropriate coefficient, resulting from the momentum equations. In 2–D problems, it is convenient to analyze simple SGs and UGs with square and equilateral triangles of unit side–lengths, as in Fig. 4. On a SG, without the extra damping of the $PWIM$, pressure values at 'odd' and 'even' nodes are decoupled. On an UG, the equivalent pattern is the decoupling of the pressure values at upright and inverted triangles.

It is a simple matter to show that in a 2–D grid, for any node P (in a SG, assume the node (i,j)) the $PWIM$ is equivalent to the following symbolic equation

$$\nabla\cdot\vec{V} = \nabla\cdot\left.\overline{\vec{V}}\right|_P - \lambda D\left[p_P + \lambda_1\sum_{nei_1}p + \lambda_2\sum_{nei_2}p\right], \tag{12}$$

where

	λ	nei_1	λ_1	nei_2	λ_2
SGs	4	(i+1,j), (i-1,j), (i,j+1), (i,j-1)	$-\frac{1}{3}$	(i+2,j), (i-2,j), (i,j+2), (i,j-2)	$\frac{1}{12}$
UGs	$\frac{\sqrt{3}}{2}$	1, 2, 3	$-\frac{1}{2}$	4, 5, 6, 7, 8, 9	$\frac{1}{12}$

By comparing the coefficients of the previous table, one may remark the similarity between the artificial diffusion support stencils in SGs and UGs. This is why pseudo–UGs (i.e. triangulated SGs) give very smooth pressure fields (see results by Thomadakis and Leschziner [8]). Smooth results, not shown here in the interest of space, have been also
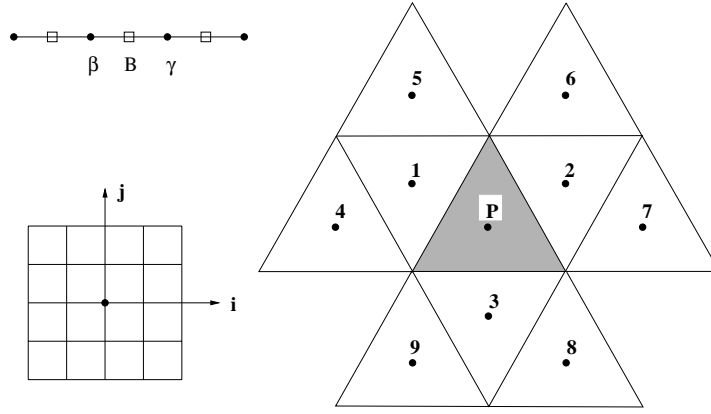
Fig. 4. Computational stencil in 1–D (left, upper) and 2–D (left, lower) structured and in 2–D unstructured grids (right) for the calculation of artificial diffusion.

obtained by the present method applied on pseudo–UGs. Nevertheless, in real UGs minor wiggles may locally appear in some irregular situations (for example when a node is surrounded by a different number of triangles than its neighbours). To improve this slight decoupling, $PWIM$ needs further investigation and there is ongoing research in this direction.

6.2 Validation

In order to isolate the boundary conditions effect on the velocity–pressure decoupling, the test cases that will be analyzed below are all using hybrid UGs, as previously defined. Computations have been performed and results are shown here for $TC1$. So, the static pressure coefficient distributions along the cylinder surface, for $Re = 20$, 40 and 100, are illustrated in Fig. (5). The pressure coefficient is defined as

$$C_P = \frac{p - p_t}{\frac{1}{2}\rho V_{inf}^2}$$

where p_t is the pressure at the front stagnation point. Computational results from Fornberg et al. [2] and the results obtained using a SG (Giannakoglou and Politis [3]) are also included in the figure. In all cases, a good agreement between calculations and the reference results is observed and the pressure field is very smooth.

The second test case examined ($TC2$) concerns the flow in NACA–12 airfoil cascade, at -10, 0 and $+10^o$ incidence angles. The cascade exhibits a unity solidity and it is placed in 30° stagger angle. In all three cases examined, the Reynolds number of the flow was equal to 1000, based on the axial velocity, the airfoil chord and the kinematic viscosity. A unique hybrid UG has been used and this is shown in Fig. (6). The structured part of the grid consists of a zone that surrounds the airfoil with four layers of triangles. In the region off the first zone, a regular unstructured grid was generated, resulting in a total number of about 10000 nodes.

In Fig. (6), the distribution of the static pressure coefficient along the airfoil is presented for all cases examined. The static pressure coefficient is defined as

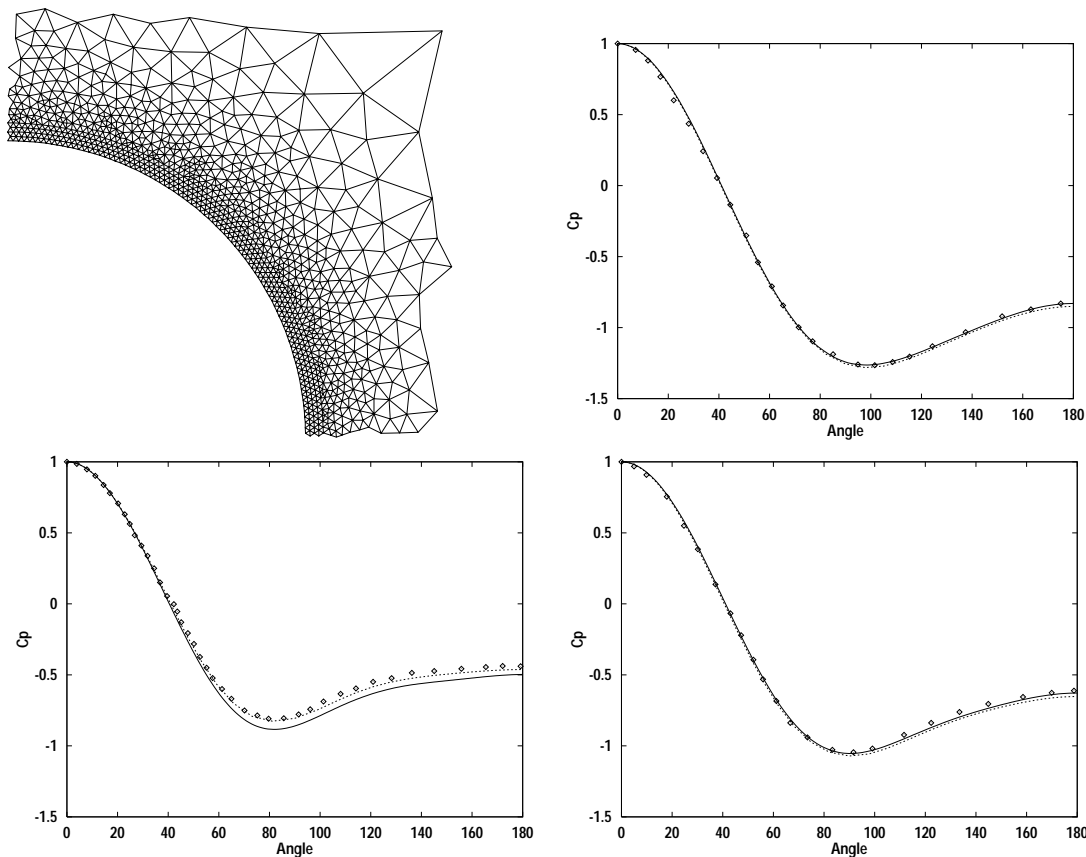$$C_P = \frac{p - p_t}{\frac{1}{2}\rho V_{\infty,ax}^2},$$

Fig. 5. Detail of the hybrid UG and computed wall–pressure distributions for $TC1$. Clockwise from top: $Re = 20$, 40 and 100. Full lines: present calculation, broken lines: Giannakoglou and Politis [3], symbols: Fornberg [2].

where p_t to the total pressure at the inlet to the cascade. The present calculations are compared with numerical predictions using a SG of 128∗21 nodes in the streamwise and the pitchwise direction respectively (Giannakoglou and Politis [4]) and the reference results of Rosenfeld and Wolfshtein [7], obtained by a vorticity–stream function method.

7. CONCLUSIONS

In this paper, a pressure–correction method for incompressible, laminar, 2–D flows using unstructured grids with triangular elements was presented. The decoupling of the pressure and velocity fields was circumvented by extending the $PWIM$, originally developed for SGs. It was shown than in real UGs, when wall–pressure boundary conditions are obtained directly from the corresponding cells' barycenters a non–smooth pressure distribution appears. This cituation was partially circumvented using hybrid UGs and finally the pressure wiggles were fully suppressed using hybrid UGs. On the other hand, it has been shown why the $PWIM$ behaves similarly on SGs and 'pseudo'–UGs, and was underlined the need for further investigation of the adequacy of the $PWIM$ for real UGs.

8. REFERENCES

[1] L. Davidson, A Pressure Correction Method For Unstructured Meshes with Arbitrary Control Volumes, *Int. J. Num. Methods in Fluids 21*, 265–281 (1996).

[2] B. Fornberg, A Numerical Study of Steady Viscous Flow Past a Circular Cylinder, *J. Fluid Mechanics 98*, 819-855 (1980).
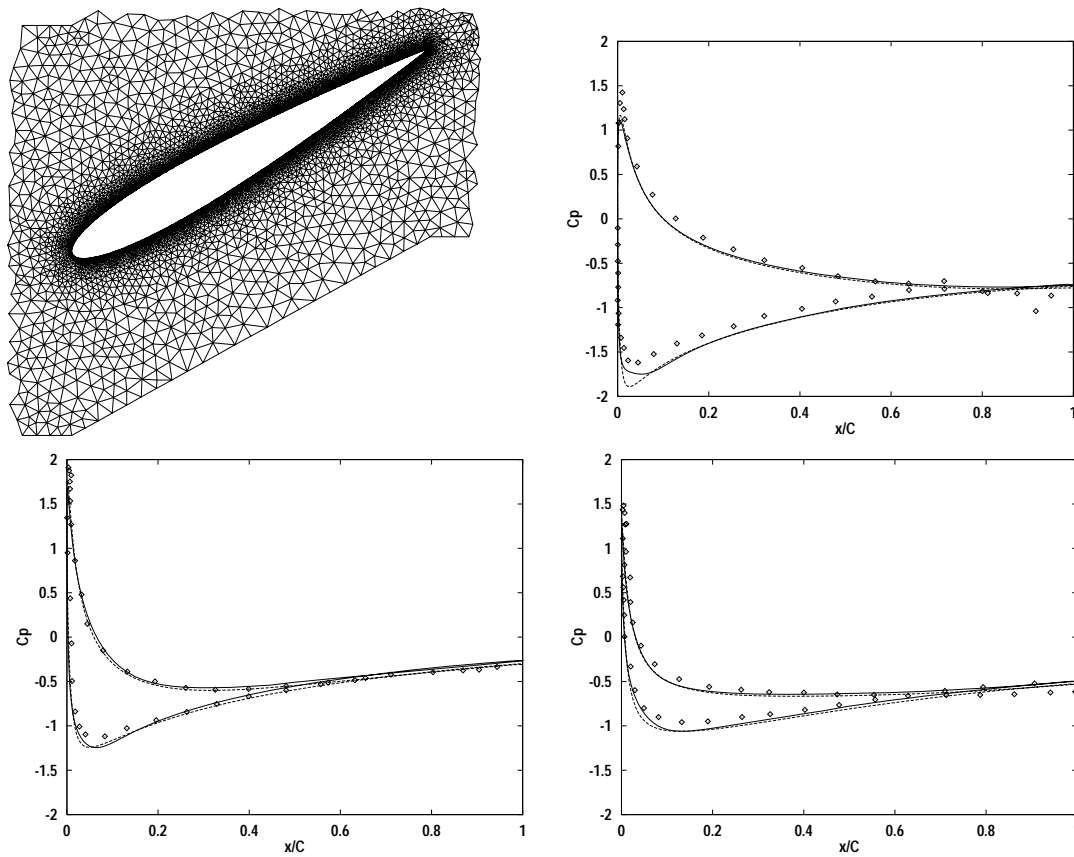
Fig. 6. Detail of the hybrid UG and computed wall–static pressure distributions for $TC2$. Clockwise from top: $i = -10^o$, $i = 0^o$ and $i = +10^o$. Full lines: present calculation, broken lines: Giannakoglou and Politis [4], symbols: Rosenfeld and Wolfshtein [7].

[3] K. C. Giannakoglou and E. S. Politis, A Segregated Implicit Solution Algorithm for 2–D and 3–D Laminar Incompressible Flows, *Int. J. Num. Methods in Fluids 21*, 1067–1086 (1995).

[4] K. C. Giannakoglou and E. S. Politis, A Pressure Correction Scheme Using Coupled Momentum Equations, *Numerical Heat Transfer 32*, 419–435 (1997).

[5] S. Majumdar, Role of Underrelaxation in Momentum Interpolation for Calculation of Flow with Nonstaggered Grids, *Num. Heat Transfer 13*, 125-132 (1988).

[6] C. M. Rhie and W. L. Chow, Numerical Study of the Turbulent Flow Past an Airfoil with Trailing Edge Separation, *AIAA Journal 21*, 1525–1532 (1983).

[7] M. Rosenfeld and M. Wolfshtein, Numerical Calculation of a Laminar Two–Dimensional Straight Cascade Flow, *Computers & Fluids 12*, 293–310 (1984).

[8] M. Thomadakis and M. A. Leschziner, A Pressure–Correction Method for the Solution of Incompressible Viscous Flows on Unstructured Grids, *Report TFD/95/05*, Department of Mechanical Engineering, UMIST (1995).